PHYSOR 2004 -The Physics of Fuel Cycles and Advanced Nuclear Systems: Global Developments
Chicago, Illinois, April 25-29, 2004, on CD-ROM, American Nuclear Society, Lagrange Park, IL. (2004)

Solution of the 1D Kinetic Diffusion Equations Using a Reduced Nodal Cubic Scheme

Armando Gómez[1], Arturo Delfín[1], Gustavo Alonso[1,2] and Edmundo del Valle[2]
[1]*Instituto Nacional de Investigaciones Nucleares, Km. 36.5 Carretera México-Toluca, Ocoyoacac, C.P. 52045, Estado de México, Mexico*
[2]*Instituto Politécnico Nacional, Av. IPN s/n, C.P. 07738, Mexico City, Mexico*

In this work it is described a novel method to solve the multi-group time-dependent diffusion equations based on a nodal cubic space interpolation in addition to the application of quadrature rules simplifying the stiffness and mass matrices arising in a finite element procedure. Numerical results for a well known benchmark problem are also provided.

KEYWORDS: Diffusion, nodal methods, reactor kinetics, quadrature rules, benchmark problems

1. Introduction

In middle 80's the 1D time-dependent diffusion equations were solved using a classical finite element technique with Lagrange interpolants [1,2]. Some time later, the same equations were solved using a collocation method with a cubic Hermite interpolant [3]. In both approaches the θ scheme for the time integration was applied. The numerical results got by that time were favorable to the collocation method due to its cubic interpolation. Here we apply a nodal cubic approximation [4] that is built up using as interpolation parameters the zero-th and first Legendre moments of the flux and its point values at the left and right edges of each cell of the discretization. To simplify stiffness and mass matrices arising in the finite element procedure some quadrature rules are applied. Several details regarding the implementation of this technique are provided as well as numerical results for a well known benchmark problem.

2. The Time-Dependent Neutron Diffusion Equations

It is well known that the time dependent multi-group diffusion equations are given by [5]:

$$\frac{1}{\mathrm{V}^{\mathrm{g}}}\frac{\partial}{\partial \mathrm{t}}\phi^{g}(x,t)=\frac{\partial}{\partial x}D^{g}(x,t)\frac{\partial}{\partial x}\phi^{g}(x,t)-\Sigma_{R}^{g}(x,t)\phi^{g}(x,t)+\sum_{g'=1}^{G}\Sigma_{s}^{g\to g'}(x,t)\phi(x,t)$$

$$+(1-\beta)\chi^{g}\sum_{g'=1}^{G}\nu^{g}\Sigma_{f}^{g'}(x,t)+\sum_{i=1}^{I}\lambda_{i}\chi_{i}^{g}C_{i}(x,t);\qquad \mathrm{g}=1,...\mathrm{G}; \tag{1}$$

and

$$\frac{\partial}{\partial \mathrm{t}}C_{i}(x,t)=\beta_{i}\sum_{g=1}^{G}\nu^{g}\Sigma_{f}^{g}(x,t)\phi^{g}(x,t)-\lambda_{i}C_{i}(x,t);\qquad i=1,...I_{p}; \tag{2}$$

where $\phi^{g}(x,t)$ is the neutron flux in the energy group *g,* and $C_{i}(x,t)$ is the neutron delayed precursors concentration for the *i*-th group of delayed neutrons. *G* and I_{p} are the total number of energy groups and of delayed precursors respectively. All the other parameters have the usual meaning [5]. The neutron fluxes must satisfy given initial and boundary conditions while concentrations of neutron delayed precursors must satisfy only given initial conditions.

3. Space Discretization Using a Finite Element Method

Typically in a finite element method $\phi^g(x,t)$ and $C_i(x,t)$ are approximated by

$$\phi^g(x,t) \equiv \sum_{k=1}^{N_f} U_k(x)\phi_k^g(t); \quad g = 1,...,\mathrm{G}; \quad \forall x \in [a,b], \qquad t \in (0,T], \tag{3}$$

$$C_i(x,t) \equiv \sum_{m=1}^{\mathrm{N_p}} V_m(x)C_i^m(t); \qquad i = 1,...,I_p; \quad \forall x \in [a,b], \qquad t \in (0,T] \tag{4}$$

where

N_f: is the number of unknowns for the neutron flux on each energy group,
N_p: is the number of unknowns for the precursors concentrations on each delayed group,
U_k: is the k-th global basis function for neutron fluxes,
V_m: is the m-th global basis function for the precursors concentrations.

If Eqs. (3) and (4) are substituted into Eqs. (1) and (2), and the resulting equations are multiplied by U_j and V_l and integrated over the whole domain Ω, then the following set of equations are obtained [1,2]:

$$\frac{M_f}{V^g}\frac{d\phi^g(t)}{dt} = -K^g\phi^g(t) - \sum_{g'=1}^{G} S^{g'\to g}\phi^{g'}(t) + (1-\beta)\sum_{g'=1}^{G} F^{gg'}\phi^{g'}(t) + \sum_{i=1}^{I} F^{gi}C_i(t); \quad g = 1,...,\mathrm{G} \tag{5}$$

$$M_p\frac{dC_i(t)}{dt} = \sum_{g'=1}^{G} P^{ig'}\phi^{g'}(t) + \lambda_i M_p C_i(t); \qquad i = 1,...,I_p \tag{6}$$

where $\phi^g(t) = \left[\phi_1^g(t),\ldots,\phi_{N_f}^g(t)\right]^T$; $g = 1,\ldots,G$; $\quad C_i(t) = \left[C_i^1(t),\ldots,C_i^{N_p}(t)\right]^T$; $\quad i = 1,\ldots,I_p$

and the elements of the matrices involved are described in Table 1.

Table 1. Definition of local matrices and their elements

Matrix	$\mathbf{N_{rows}}$ **x** $\mathbf{N_{columns}}$	Matrix elements
M_f	$N_f \times N_f$	$m_{f,ij} \equiv \int_\Omega U_i(x)U_j(x)dx$
M_p	$N_p \times N_p$	$m_{p,ij} \equiv \int_\Omega \mathrm{V}_i\mathrm{V}_j dx$
K^g	$N_f \times N_f$	$k_{ij}^g \equiv \int_\Omega D^g \nabla U_i \cdot \nabla U_j dx$
$S^{g'\to g}$	$N_f \times N_f$	$s_{ij}^{g'\to g} \equiv \int_\Omega \Sigma^{g'\to g} U_i U_j dx$
$F^{gg'}$	$N_f \times N_f$	$f_{ij}^{gg'} \equiv \chi^g \int_\Omega \nu^{g'}\Sigma_f^{g'} U_i U_j dx$
F^{gi}	$N_f \times N_p$	$f_{jk}^{gi} \equiv \lambda_i \chi_i^g \int_\Omega U_j \mathrm{V}_k dx$
$P^{ig'}$	$N_p \times N_f$	$p_{jk}^{ig'} \equiv \beta_i \int_\Omega \nu^{g'}\Sigma_f^{g'}\mathrm{V}_j U_k dx$

3.1 The Nodal Finite Element Method (Polynomial Interpolation)

Nodal finite element methods in 1D are based in the interpolation of the dependent variables not only in specific points as it is the classical case but also in the interpolation of cell Legendre moments that are defined in the reference cell [-1,+1] in the following way [4]:

$$\phi_C^i = \frac{2i+1}{2}\int_{-1}^{1} P_i(x)\phi(x)dx \qquad i = 0,1,2,\ldots \tag{7}$$

where $P_i(x)$ is the Legendre polynomial of degree i. Thus, in a general case, a nodal element of degree k will have k-1 cell Legendre moments. In particular, in the cubic case (k = 3) there will be two basis functions associated to cell Legendre moments and another two to the left and right edges of a cell. Basis functions are given in this case by [4]:

$$u_l(\xi) = \frac{1}{2}\left[P_2(\xi) - P_3(\xi)\right] \tag{8a}$$

$$u_C^0(\xi) = P_0(\xi) - P_2(\xi) \tag{8b}$$

$$u_C^1(\xi) = P_1(\xi) - P_3(\xi) \tag{8c}$$

$$u_r(\xi) = \frac{1}{2}\left[P_2(\xi) + P_3(\xi)\right] \tag{8d}$$

3.2 Computation of Matrix Elements Using Quadrature Rules

Once that a set of basis functions have been defined it is useful to use quadrature rules (QR) to evaluate numerically the matrix elements if they provide some benefits. In this work such evaluation was carried out using two different quadrature rules. The first one was the 3-points Gauss-Radau [6]. Integrals of products of basis functions were evaluated with this quadrature that allows to lump the elementary mass matrix in such a way that only two of its elements are non-zero and it is given by:

$$\hat{m} = \frac{1}{3}\begin{bmatrix} 0 & 0 & 0 & 0 \\ 0 & +6 & 0 & 0 \\ 0 & 0 & +2 & 0 \\ 0 & 0 & 0 & 0 \end{bmatrix} \tag{9}$$

The second QR was a non-standard 4-points Newton-Cotes [6] to evaluate the integrals of products of first derivatives of the basis functions. The result of applying this QR leads to the following stiffness matrix:

$$\hat{k} = \begin{bmatrix} +3 & -3 & +2 & 0 \\ -3 & +6 & 0 & -3 \\ +2 & 0 & +4 & -2 \\ 0 & -3 & -2 & +3 \end{bmatrix} \tag{10}$$

4. Time Integration

Once that the space discretization has been done, then Eqs. (5) and (6) will be a set of N_fG+N_pI ordinary differential equations. Thus, the next step is to carry out the time discretization over the time domain $(0,T]$. One of the ways to do that is by integrating those equations over the interval $[t_j,t_{j+1}]$ approximating the integrals with the θ method as follows:

$$\int_{t_j}^{t_{j+1}} f(t)dt = \Delta t\left[\theta f_{j+1} + (1-\theta) f_j\right] \tag{11}$$

Particular choices of the θ parameter lead to well known discretization schemes in time. For instance, if θ =1/2, the Crank-Nicolson scheme is obtained, if θ =1 then the backward Euler

scheme is obtained. Two θ parameters were introduced in the time discretization, namely θ_f and θ_p, associated to the neutron flux and to precursor concentrations respectively. Therefore, after integrating Eqs. (5) and (6) over the time interval $[t_j, t_{j+1}]$ using the θ method the following algebraic system is obtained [1,2]:

$$A_{j+1}\underline{\psi}_{j+1} = \underline{S}_j;\ j = 0,1,2,\ldots \tag{12}$$

where

$\underline{\psi}_{j+1} = \left[\underline{\phi}^1_{j+1},\ldots,\underline{\phi}^G_{j+1},\underline{C_1}^{j+1},\ldots,\underline{C_{I_p}}^{j+1}\right]^T$ and $\underline{S}_j = \left[\underline{S}^1_j,\ldots,\underline{S}^G_j,\underline{S}^j_1,\ldots,\underline{S}^j_{I_p}\right]^T$ are the vector of unknowns at time t_{j+1} and the source term vector at time t_j.

The order of matrix A_{j+1} is $N_f G + N_p I_p$. Due to space limitations full details are not given but the readers are invited to see Refs. [1,2].

To solve Eqn. (12) firstly it is necessary to know the neutron flux and precursor concentrations at time t_j. With this information the right hand side vector is built up and finally the system can be solved to obtain the neutron flux and precursor concentrations at time t_{j+1}. However matrix A_{j+1} is not symmetric and if cubic elements are used then its total band-width would be $W_T^A = 2(N_f G + (I_p - 1)N_p + N_e) - 1$. Figure 1 shows the structure of matrix A_{j+1} in the particular case $N_e = 5$, $G = 2$, and $I_p = 1$.

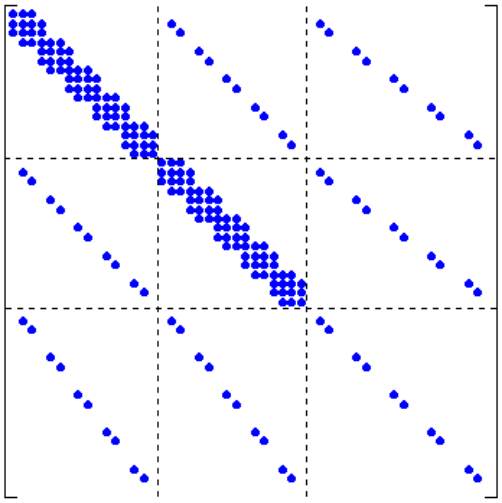

Fig. 1 Distribution of non-zero elements of matrix A_{j+1} using $N_e = 5$, $G = 2$, and $I_p = 1$.

Taking into account that precursors concentrations at time t_{j+1} can be expressed in terms of neutron flux at times t_j and t_{j+1}, and the precursors concentrations at time t_j then a simplified algebraic system having only the neutron flux at time t_{j+1} as unknowns is obtained

$$B_{j+1}\underline{\phi}_{j+1} = \underline{Q}_j \tag{13}$$

with

$\underline{\phi}_{j+1} = \left[\underline{\phi}^1_{j+1},\ldots,\underline{\phi}^G_{j+1}\right]^T$ and $\underline{Q}_j = \left[\underline{S}^1_{f,j},\ldots,\underline{S}^G_{f,j}\right]^T$

where now matrix B_{j+1} is of order $(kN_e+1)G$ (in this work k = 3) and its total band-width is $W_T^B = 2(kN_e+1)(G-1)+1$. Figure 2 shows the structure of this matrix for $N_e = 5$, $G = 2$, and I_p = 1.

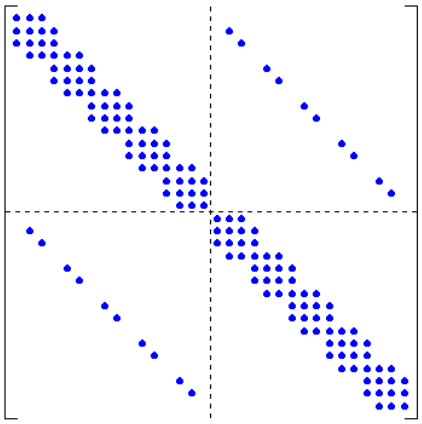

Fig. 2 Distribution of non-zero elements of matrix B_{j+1} using $N_e = 5$, $G = 2$, and $I_p = 1$.

Here it is important to point out that elementary matrices (9) and (10) lead to interesting global structure that decouples the left and right flux unknowns on each cell. This in turn allows to express those unknowns in terms of the zeroth and first Legendre moments of the flux and if they are substituted in the remaining equations then a new algebraic system is obtained which unknowns are only the zeroth and first Legendre moments of the flux for each energy group and cell and it is given by

$$a_{j+1}\underline{\phi}_{j+1} = \underline{q}_j \tag{14}$$

where matrix a_{j+1} is of order $2N_eG$ and its structure is shown in Figure 3a.

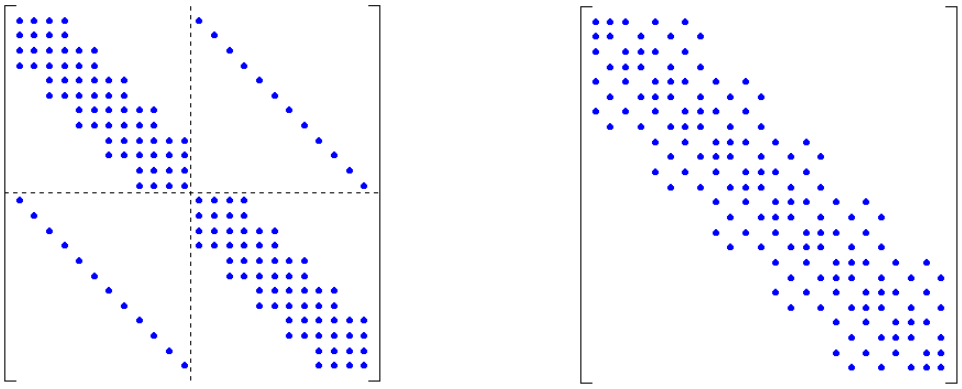

(a) (b)

Fig. 3 Distribution of non-zero elements of matrix a_{j+1} using $N_e = 5$, $G = 2$, and $I_p = 1$.

The generic form of the of the elements of the vector $q_{i,j}^{\ell g}$ and equations corresponding to the algebraic system (14) for the energy group g and case θ=1, are the following

$$q_{i,j}^{\ell g} = \frac{1}{(2\ell+1)V^g}\phi_{i,j}^{\ell g} + h_j\frac{\Delta x_i}{2\ell+1}\chi^g\sum_{k=1}^{Ip}\frac{\lambda_k C_{k,j}^{\ell}}{1+h_j\lambda_k},\ \ \ell = 0,1,\ g = 1,...,G \tag{15}$$

$$
\begin{aligned}
&a^{00g}_{i-1,j+1}\phi^{0g}_{i-1,j+1}+a^{01g}_{i-1,j+1}\phi^{1g}_{i-1,j+1}+a^{00g}_{i,j+1}\phi^{0g}_{i,j+1}+a^{01g}_{i,j+1}\phi^{1g}_{i,j+1}+a^{00g}_{i+1,j+1}\phi^{0g}_{i+1,j+1}+a^{01g}_{i+1,j+1}\phi^{1g}_{i+1,j+1}-\\
&h_j\Delta x_i\sum_{g'=1}^{G}{}'\Sigma^{g'\to g}_{si,j+1}\phi^{0g'}_{i,j+1}-h_j\Delta x_i\chi^g\sum_{g'=1}^{G}{}'\nu\Sigma^{g'}_{fi,j+1}\phi^{0g'}_{i,j+1}=q^{0g}_{i,j}\\
&a^{10g}_{i-1,j+1}\phi^{0g}_{i-1,j+1}+a^{11g}_{i-1,j+1}\phi^{1g}_{i-1,j+1}+a^{10g}_{i,j+1}\phi^{0g}_{i,j+1}+a^{11g}_{i,j+1}\phi^{1g}_{i,j+1}+a^{10g}_{i+1,j+1}\phi^{0g}_{i+1,j+1}+a^{11g}_{i+1,j+1}\phi^{1g}_{i+1,j+1}-\\
&h_j\frac{\Delta x_i}{3}\sum_{g'=1}^{G}{}'\Sigma^{g'\to g}_{si,j+1}\phi^{1g'}_{i,j+1}-h_j\frac{\Delta x_i}{3}\chi^g\sum_{g'=1}^{G}{}'\nu\Sigma^{g'}_{fi,j+1}\phi^{1g'}_{i,j+1}=q^{1g}_{i,j}
\end{aligned}
\tag{16}
$$

where each one of the matrix elements are defined by

$$
a^{00g}_{i-1,j+1}=-6h_j\frac{D^g_{i-1,j+1}D^g_{i,j+1}}{\Delta x_iD^g_{i-1,j+1}+\Delta x_{i-1}D^g_{i,j+1}},\ a^{01g}_{i-1,j+1}=-4h_j\frac{D^g_{i-1,j+1}D^g_{i,j+1}}{\Delta x_iD^g_{i-1,j+1}+\Delta x_{i-1}D^g_{i,j+1}},
\tag{17a}
$$

$$
\begin{aligned}
a^{00g}_{i,j+1}=&\frac{1}{V^g}+h_j\Delta x_i\Sigma^g_{Ri,j+1}+12h_j\frac{D^g_{i,j+1}}{\Delta x_i}-h_j\Delta x_i(1-\beta)\chi^g\nu\Sigma^g_{fi,j+1}-\\
&-6h_j\frac{\Delta x_{i-1}}{\Delta x_i}\frac{D^{g2}_{i,j+1}}{\Delta x_iD^g_{i-1,j+1}+\Delta x_{i-1}D^g_{i,j+1}}-6h_j\frac{\Delta x_{i+1}}{\Delta x_i}\frac{D^{g2}_{i,j+1}}{\Delta x_iD^g_{i+1,j+1}+\Delta x_{i+1}D^g_{i,j+1}},
\end{aligned}
\tag{17b}
$$

$$
a^{01g}_{i,j+1}=4h_j\frac{\Delta x_{i-1}}{\Delta x_i}\frac{D^{g2}_{i,j+1}}{\Delta x_iD^g_{i-1,j+1}+\Delta x_{i-1}D^g_{i,j+1}}-4h_j\frac{\Delta x_{i+1}}{\Delta x_i}\frac{D^{g2}_{i,j+1}}{\Delta x_iD^g_{i+1,j+1}+\Delta x_{i+1}D^g_{i,j+1}},
\tag{17c}
$$

$$
a^{00g}_{i+1,j+1}=-6h_j\frac{D^g_{i,j+1}D^g_{i+1,j+1}}{\Delta x_{i+1}D^g_{i,j+1}+\Delta x_iD^g_{i+1,j+1}},\ a^{01g}_{i+1,j+1}=4h_j\frac{D^g_{i,j+1}D^g_{i+1,j+1}}{\Delta x_{i+1}D^g_{i,j+1}+\Delta x_iD^g_{i+1,j+1}},
\tag{17d}
$$

$$
a^{10g}_{i-1,j+1}=4h_j\frac{D^g_{i-1,j+1}D^g_{i,j+1}}{\Delta x_iD^g_{i-1,j+1}+\Delta x_{i-1}D^g_{i,j+1}},\ a^{11g}_{i-1,j+1}=\frac{8}{3}h_j\frac{D^g_{i-1,j+1}D^g_{i,j+1}}{\Delta x_iD^g_{i-1,j+1}+\Delta x_{i-1}D^g_{i,j+1}},
\tag{17e}
$$

$$
a^{10g}_{i,j+1}=4h_j\frac{\Delta x_{i-1}}{\Delta x_i}\frac{D^{g2}_{i,j+1}}{\Delta x_iD^g_{i-1,j+1}+\Delta x_{i-1}D^g_{i,j+1}}-4h_j\frac{\Delta x_{i+1}}{\Delta x_i}\frac{D^{g2}_{i,j+1}}{\Delta x_iD^g_{i+1,j+1}+\Delta x_{i+1}D^g_{i,j+1}},
\tag{17f}
$$

$$
\begin{aligned}
a^{11g}_{i,j+1}=&\frac{1}{3V^g}-h_j\frac{\Delta x_i\Sigma^g_{Ri,j+1}}{3}+8h_j\frac{D^g_{i,j+1}}{\Delta x_i}-h_j\frac{\Delta x_i}{3}(1-\beta)\chi^g\nu\Sigma^g_{fi,j+1}-\\
&-\frac{8}{3}h_j\frac{\Delta x_{i-1}}{\Delta x_i}\frac{D^{g2}_{i,j+1}}{\Delta x_iD^g_{i-1,j+1}+\Delta x_{i-1}D^g_{i,j+1}}-\frac{8}{3}h_j\frac{\Delta x_{i+1}}{\Delta x_i}\frac{D^{g2}_{i,j+1}}{\Delta x_iD^g_{i+1,j+1}+\Delta x_{i+1}D^g_{i,j+1}},
\end{aligned}
\tag{17g}
$$

$$
a^{10g}_{i+1,j+1}=-4h_j\frac{D^g_{i,j+1}D^g_{i+1,j+1}}{\Delta x_{i+1}D^g_{i,j+1}+\Delta x_iD^g_{i+1,j+1}},\ a^{11g}_{i+1,j+1}=\frac{8}{3}h_j\frac{D^g_{i,j+1}D^g_{i+1,j+1}}{\Delta x_{i+1}D^g_{i,j+1}+\Delta x_iD^g_{i+1,j+1}},
\tag{17h}
$$

Up to this point, the size of matrix a_{j+1} is less than the one of matrix B_{j+1}, but it is still possible to reduce the computing time by applying a group-moments reordering [1,2]. This reduces the total band-width of matrix a_{j+1} to $W_T^{aR}=2(k-1)G+1$. Figure 3b shows how are now distributed the non-zero elements of a_{j+1}. Once that the algebraic system is solved for the Legendre moments of the neutron flux in a given time-step then the precursors concentrations are computed at t_{j+1}. This completes the whole calculation for the time interval $[t_j,t_{j+1}]$ and it is

repeated up to sweep the time domain *(0,T]*. The computer program McKin based in this reduced cubic nodal scheme was developed and in the next section numerical results for a well known benchmark problem are given.

5. Numerical Results (ANL Benchmark Problem 6-A3)

To test the scheme hereabove described we solved three benchmark problems. All of them are fully described in [7] but due to space limitations we show here only the numerical results for the most difficult of them, namely: the benchmark problem 6.A-3. This problem consists in a three-region slab reactor considering two-energy groups and six delayed groups. The transient starts with a linear decrease of 5% in 0.01 secs. of the thermal removal cross section in region 1 (0<x<40cm). After this time the value of the cross section is constant. Table I contains for this problem the powers per region and also the normalized total power. Figure 1 shows the thermal flux at three different times using a time step of $\Delta t = 10^{-5}$ secs. and a mesh size of 2 cm. In this work only numerical results will be given for the case θ=1/2. Table 2 shows numerical results from Ref. [7] for this benchmark and the ones obtained with McKin are shown in Table 3.

Table 2. Numerical results for the benchmark problem 6.A-3 with a finite differences method a mesh size of 2 cm and $\Delta t = 10^{-5}$ sec. [7].

Time (sec)	Relative power per region			Total Power
	Region 1	Region 2	Region 3	
0.000	1.000	1.000	1.000	1.000
0.001	1.058	1.014	1.000	1.022
0.005	2.484	1.544	1.017	1.659
0.010	3.481×10^{1}	1.258×10^{1}	1.342	1.565×10^{1}
0.015	1.570×10^{3}	5.388×10^{2}	1.485×10^{1}	6.803×10^{2}
0.020	6.954×10^{4}	2.385×10^{4}	6.179×10^{2}	3.011×10^{4}

Table 3. Numerical results obtained with McKin (6.A-3), for a mesh size of 2 cm, and $\Delta t = 10^{-5}$ seg.

Time (sec)	Relative power per region			Total Power
	Region 1	Region 2	Region 3	
0.000	1.000	1.000	1.000	1.000
0.001	1.058	1.014	1.000	1.022
0.005	2.481	1.543	1.017	1.658
0.010	3.459×10^{1}	1.250×10^{1}	1.340	1.555×10^{1}
0.015	1.547×10^{3}	5.310×10^{2}	1.466×10^{1}	6.703×10^{2}
0.020	6.796×10^{4}	2.331×10^{4}	6.041×10^{2}	2.943×10^{4}

Figure 4 shows the thermal neutron flux obtained with McKin at $t = 0, 0.01$ and 0.02 seconds using a $\Delta t = 10^{-5} s$. and a mesh size of 2 cm.

6. Conclusions

A new mesh-centered finite differences technique has been developed from a cubic nodal approximation and applied in the numerical solution of the 1D multi-group time-dependent diffusion equations. The technique arises from a combination of quadrature rules allowing to

simplify stiffness and mass matrices in such a way that the original algebraic system can be reduced to a new having only the Legendre moments of the neutron flux as unknowns. Although there is no evidence regarding the accuracy of the technique it is expected a continuous order 4 in space due mainly to two aspects, namely: the degree of the polynomial approximation and the accuracy of the QRs. The numerical results obtained are similar to the ones of the benchmark problem. They are not exactly the same because they were obtained using a low order finite-differences technique.

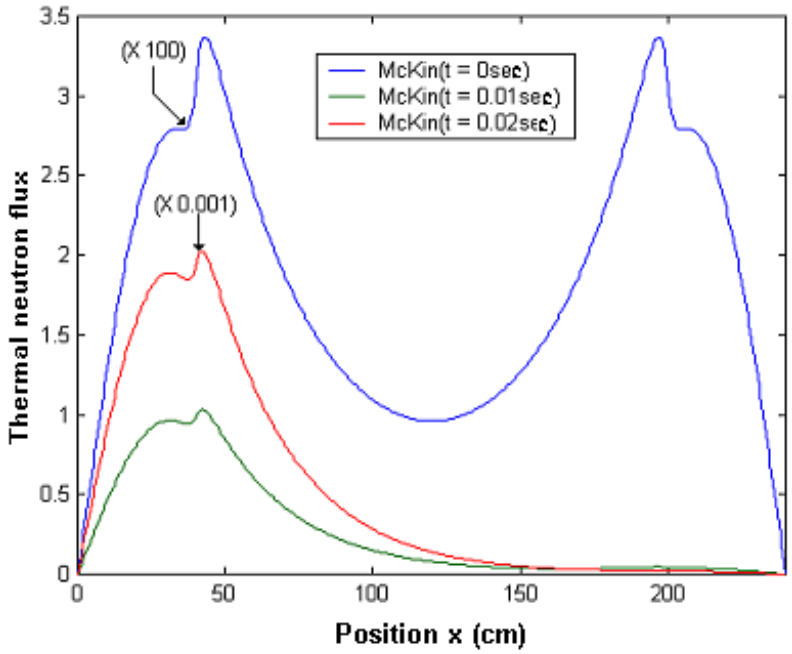

Fig. 4 Thermal flux obtained with McKin at $t = 0,\ 0.01$ and 0.02 secs. using $\Delta t = 10^{-5}\, s$, and a mesh size of 2 cm.

Acknowledgements

The authors acknowledge the support given by the Mexican Science and Technology Research Council (CONACyT) through the research project 33806-U.

References

1) E. Del Valle, "Aplicación del Método de Elementos Finitos a la Dinámica de Reactores Nucleares", *MSc Thesis*, Instituto Politécnico Nacional, México (1981).
2) E. del Valle, "Application of the Galerkin Finite Element Method to Reactor Dynamic Problems", *Transport Theory and Statistical Physics,* **12**(3), 251 (1983).
3) D. Meade, "Collocation Methods for Space Time Nuclear Reactor Dynamics", *PhD Thesis*, University of California, Berkeley (1982).
4) J.P. Hennart and E. del Valle, "A generalized nodal finite element formalism for discrete ordinates equations in slab geometry. Part I: theory in the continuous moment case", *Transport Theory and Statistical Physics,* **2**(10) (1992).
5) J.J. Duderstadt and L. J. Hamilton, Nuclear Reactor Analysis, John Willey & Sons (1976).
6) P.J. Davis and P. Rabinowitz, *Methods of Numerical Integration*, Academic Press (1984).
7) Benchmark Book Problem ANL-7416, Supplement 2, Argonne National Laboratory, (1977).